Influence of labeling parameters and respiratory motion on velocity-selective arterial spin labeling for renal perfusion imaging

Bones, I.K.; Franklin, S.L.; Harteveld, A.A.; Osch, M.J.P. van; Hendrikse, J.; Moonen, C.; ... ; Bos, C.

Magnetic Resonance in Medicine

Influence of labeling parameters and respiratory motion on velocity-selective arterial spin labeling for renal perfusion imaging

Isabell K. Bones[1] 🔘 | Suzanne L. Franklin[1,2] 🔘 | Anita A. Harteveld[1] 🔘 |
Matthias J. P. van Osch[2] 🔘 | Jeroen Hendrikse[3] 🔘 | Chrit Moonen[1] 🔘 |
Marijn van Stralen[1] 🔘 | Clemens Bos[1] 🔘

[1]Center for Image Sciences, University Medical Center Utrecht, Utrecht, the Netherlands

[2]C.J. Gorter Center for High Field MRI, Department of Radiology, Leiden University Medical Center, Leiden, the Netherlands

[3]Department of Radiology, University Medical Center Utrecht, Utrecht, the Netherlands

Correspondence
Isabell K. Bones, Center for Image Sciences, University Medical Center Utrecht, Heidelberglaan 100, 3584 CX Utrecht, the Netherlands.
Email: i.k.bones@umcutrecht.nl

Purpose: Arterial transit time uncertainties and challenges during planning are potential issues for renal perfusion measurement using spatially selective arterial spin labeling techniques. To mitigate these potential issues, a spatially non-selective technique, such as velocity-selective arterial spin labeling (VSASL), could be an alternative. This article explores the influence of VSASL sequence parameters and respiratory induced motion on VS-label generation.

Methods: VSASL data were acquired in human subjects ($n = 15$), with both single and dual labeling, during paced-breathing, while essential sequence parameters were systematically varied; (1) cutoff velocity, (2) labeling gradient orientation and (3) post-labeling delay (PLD). Pseudo-continuous ASL was acquired as a spatially selective reference. In an additional free-breathing single VSASL experiment ($n = 9$) we investigated respiratory motion influence on VS-labeling. Absolute renal blood flow (RBF), perfusion weighted signal (PWS), and temporal signal-to-noise ratio (tSNR) were determined.

Results: (1) With decreasing cutoff velocity, tSNR and PWS increased. However, undesired tissue labeling occurred at low cutoff velocities (≤ 5.4 cm/s). (2) Labeling gradient orientation had little effect on tSNR and PWS. (3) For single VSASL high signal appeared in the kidney pedicle at PLD < 800 ms, and tSNR and PWS decreased with increasing PLD. For dual VSASL, maximum tSNR occurred at PLD = 1200 ms. Average cortical RBF measured with dual VSASL (264 ± 34 mL/min/100 g) at a cutoff velocity of 5.4 cm/s, and feet-head labeling was slightly lower than with pseudo-continuous ASL (283 ± 55 mL/min/100 g).

Conclusion: With well-chosen sequence parameters, tissue labeling induced by respiratory motion can be minimized, allowing to obtain good quality RBF maps using planning-free labeling with dual VSASL.

KEYWORDS

arterial spin labeling, kidney function, motion artifacts, renal perfusion, velocity-selective labeling

1 | INTRODUCTION

Renal perfusion has been proposed as an indicator for kidney function.[1] To assess renal perfusion, several methods are available in the field of medical imaging, including dynamic contrast enhanced (DCE) MRI.[1,2] While MRI is harmless, DCE-MRI requires the injection of a contrast agent. With these injections, concerns for several patient populations arise, for example those with poor renal clearance, those who require repeated evaluations of renal function, and the pediatric population.

Over the past decades, a non-invasive alternative to measure renal perfusion has been successfully demonstrated: arterial spin labeling MRI (ASL).[3] It uses magnetically labeled protons in the blood as an endogenous contrast agent. Commonly applied ASL techniques label blood spatially selectively, which then perfuses the target organ prior to measurement.[4] Although spatially selective ASL techniques have been successfully applied in the kidneys, they also have limitations. First, they require dedicated planning of the labeling slab, which can be time consuming and possibly lowering measurement repeatability, especially at higher field strength where field inhomogeneities are more pronounced.[5-7] Second, they are sensitive to the arterial transit time (ATT), the time necessary for labeled blood to flow from the labeling location into the tissue. This means that changes in upstream vasculature can bias the apparent perfusion values. ATT can be altered by several factors that influence vasculature, such as age, gender,[8,9] and current health status, as in the case of renal artery stenosis, which is suspected to both reduce renal blood flow (RBF) and increase ATT.[10] In fact, for precise perfusion quantification using ASL, it is important to correct for ATT differences.[7,11] One approach that can mitigate ATT effects and simplify planning was recently proposed: spatially non-selective ASL techniques, which label blood based on velocity; velocity-selective ASL (VSASL).[12-14]

Thus far, VSASL has mainly been demonstrated for perfusion measurement in the brain.[13,15,16] Other recent applications have included the heart[17] and the placenta.[18] To our knowledge, as yet its application for renal perfusion measurement has not been studied. This application is not trivial, knowing that the renal hemodynamics include a broad range of flow velocities in varying directions. Also, measurement errors induced by bulk motion of tissue due to (respiratory) motion could corrupt the VSASL signal.

In this study, the influence of essential VS sequence parameters (labeling cutoff velocity [V_c], labeling gradient orientation and post-labeling delay [PLD]) that potentially affect VS-label generation and label dynamics in the kidneys is studied. Repeatability is evaluated for selected settings and its sensitivity to renal perfusion is investigated by comparison with a commonly used spatially selective reference technique, pseudo-continuous ASL (pCASL). Moreover, possible influence of respiratory induced motion on the VS-label generation is investigated. Finally, suggestions for a practical implementation are provided.

2 | THEORY

2.1 | VS-label preparation & bulk motion

The idea of VSASL is to label blood by saturating (or inverting) spins that flow faster than a set cutoff velocity V_c for the label condition, whereas the blood magnetization remains untouched for the control condition. After a 90° pulse, flow sensitization is achieved by applying bipolar gradients in combination with refocusing radiofrequency (RF) pulses, such that moving spins experience different phase accrual than stationary ones before the tip-up pulse.[13] Essential for saturation of blood is that the velocity distribution is broad enough. For laminar flow inside a vessel, which has a parabolic flow profile with center velocity V_{max}, this phase modulation creates a range of phases that results in magnetization saturation of blood if it exceeds the cutoff velocity V_c (Figure 1A). The longitudinal magnetization modulation is given by

$$M_z = \pi \cdot \rho \cdot \text{sinc}\left(c \cdot V_{max}\right)$$

with $c = 2 \cdot \gamma \cdot G \cdot T$ and ρ the proton density of tissue, γ the gyromagnetic ratio, G the maximum gradient strength, and T the time between gradients with the same polarity.

Since in VSASL label is generated based on velocity, one might wonder whether bulk motion will not induce subtraction artifacts, which would make VSASL less suitable for body applications compared with cerebral perfusion imaging.
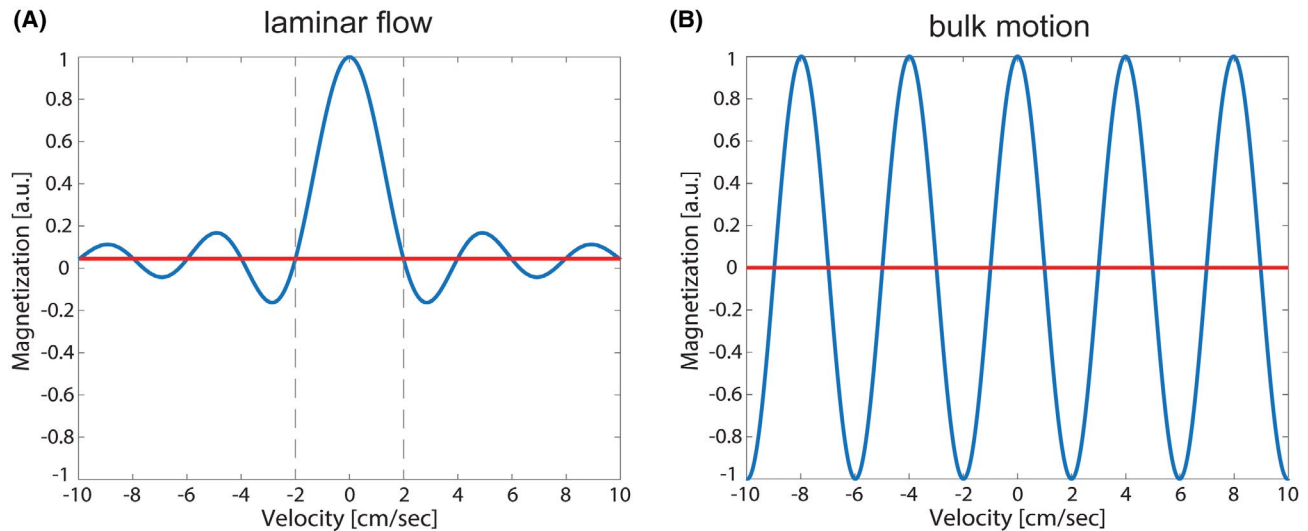
(A) laminar flow

(B) bulk motion

FIGURE 1 Simulated longitudinal magnetization modulation for a velocity range from −10 to 10 cm/s (sign as an indicator for flow directionality) for laminar flow distribution in a vessel, with the first zero crossing indicating the cutoff velocity of 2 cm/s (A) and in case of bulk motion as induced by, eg, respiratory motion (B)

For tissue of moving organs, the laminar flow velocity distribution is not present, instead the tissue moves as a whole with a single velocity. The result is a longitudinal magnetization that depends on the velocity:

$$M_z = \pi \cdot \rho \cdot \cos(c \cdot V)$$

Rather than saturation above a cutoff velocity V_c there are certain velocities V_{bulk}, for which moving spins are saturated or inverted (Figure 1B). Therefore, in addition to the desired saturation of blood flowing above the cutoff velocity (thereby creating label), an additional modulation of tissue M_z in the label image is created. Consequently, after subtraction from the control image, subtraction artifacts might appear in the perfusion images, superimposed on the typical low signal perfusion pattern.

3 | METHODS

First, the performance of VSASL was evaluated with varying VS-labeling parameter combinations and compared with the commonly used spatially selective pCASL approach. In a second experiment, the effect of respiratory motion on the generated VS-label was studied.

3.1 | VS-label preparation

VS-labeling was implemented using a pair of spatially non-selective hard 90° pulses with two adiabatic 180° refocusing pulses and bipolar gradients, with one VS-labeling module consisting of a four-gradient-pulse scheme, as illustrated in Figure 2A.[13] Such flow-sensitizing gradients will also introduce some diffusion attenuation of the ASL signal with $A_{diffusion} = 1 - e^{-b \cdot ADC_{kidney}}$[19] that depends on the b-value of the gradient-scheme, $b = \gamma^2 \cdot G^2 \cdot \delta^2 \cdot (\Delta - \delta/3)$, and the tissue apparent diffusion coefficient, $ADC_{kidney} = 2.26 \cdot 10^{-3} mm^2/s$[20] (see Table 1 for b-values and resulting error per V_c). To minimize diffusion effects the VS-labeling module duration was kept short. For a square gradient, $V_c = \pi/(\gamma \cdot G \cdot \delta \cdot (\Delta + \Delta'))$[21] where δ is the gradient duration, Δ the time between the first and the fourth gradient and Δ' the time between second and third gradient; V_c was varied by changing gradient strength G (Table 1).

The orientation of the flow-sensitizing gradients defines in which direction blood should flow to experience spin dephasing. In our implementation, the imaging slab and the flow-sensitizing gradients share the same coordinate system, hence, our referencing to the gradient orientation, viz. feet-head (FH), right-left (RL) and anterior-posterior (AP), is relative to the imaging slab angulation. The VS-labeling efficiency α_{VS} is mainly determined by T_2-decay during label[13]: $\alpha_{VS} = e^{-TE_{VS}/T_{2b}}$, where TE_{VS} is the duration of a single VS-labeling module and T_{2b} is T_2 of arterial blood (290 ms at 1.5 T).[22] In single VSASL (sVSASL) flow-sensitizing gradients are applied in the label condition to saturate blood in vessels with $V_{max} > V_c$, whereas in the control condition those gradients are turned off but the RF pulses are still played. Dual VSASL (dVSASL) contains a second VS-labeling module which is applied right before image acquisition in both label and control condition, which eliminates signal of blood accelerating above V_c after the first VS-labeling module, ie, undesired venous signal and allows quantification of RBF[14]; Figure 2B. However, the

(A) VS-module

(B) dual VSASL pulse sequence
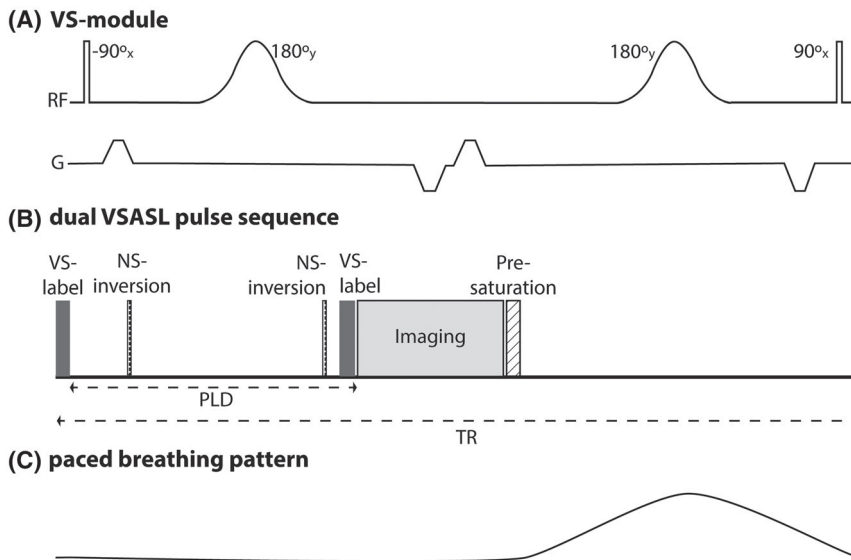
(C) paced breathing pattern

FIGURE 2 (A) The pulse sequence diagram for one VS-labeling module. (B) Dual VSASL sequence timings for one TR. A VS-labeling module at the start of the sequence is followed by a post-labeling delay, during which two non-selective inversions for BGS are applied and right before image acquisition a second VS-labeling module is played (for single VSASL this module is not played). The sequence ends with a pre-saturation to stabilize residual magnetization modulation for the following measurements. (C) Paced breathing pattern

TABLE 1 VS-labeling module settings for variations of the VS-labeling parameter cutoff velocity, V_c, with the resulting b-values from the applied VS-gradients and the expected subtraction error due to diffusion during a single VS-labeling module

Setting	V_c [cm/s]	T_{VS} [ms]	δ [ms]	Δ [ms]	G [mT/m]	b-value [s/mm^2]	1-exp(-b · ADC) [cortex, %]
1	2.1	60	0.771	39	18.00	5.34	1.20
2	5.4	60	0.771	39	7.10	0.83	0.19
3	10.7	60	0.771	39	3.57	0.21	0.05
4	16.1	60	0.771	39	2.38	0.09	0.02

second module will also attenuate the ASL signal due to additional T_2 relaxation and diffusion weighting. Pre-saturation and a long repetition time (TR) served to stabilize residual magnetization modulation from previous ASL repetitions.

3.2 | Image acquisition

All data were acquired on a 1.5T MR-system (Ingenia, Philips, The Netherlands) using a 28-element phased-array receiver-coil. A single-shot gradient echo EPI 2D multi-slice readout was used with 80 × 81 acquisition matrix; EPI factor of 55; parallel imaging factor 1.5 (SENSE) and a phase-encoding bandwidth of 30.9 Hz/pixel. In ascending order (AP), seven coronal-oblique slices were acquired with a slice gap of 1 mm, covering both kidneys with a 244 × 244 mm field of view (FOV) and an acquired voxel size of 3.05 × 2.99 × 6 mm^3. Phase encoding and SENSE direction was FH, and saturation slabs superior and inferior to the imaging volume were used to suppress undesired signal aliasing. A spectrally selective partial inversion pulse (SPIR) was used for fat suppression.

All ASL measurements consisted of 15 label-control pairs. Angulation of the imaging volume parallel to the back muscle (psoas major) minimized through-plane motion of

the kidneys; angulation average 19°, range: 11-24°. For comparison, pCASL data were acquired in each subject using balanced[23] pseudo-continuous labeling. The labeling plane was carefully planned to avoid susceptibility artifacts that could influence pCASL labeling efficiency[7] and to avoid undesired labeling of the kidneys by making sure they would not move into the labeling slab during respiration. This was achieved by staying well below the diaphragm while placing the label slab as high as possible inside the FOV as illustrated in Supporting Information Figure S6. B_0-shimming for the readout module was performed for the entire FOV. The pCASL labeling slab was shimmed separately, using automated shim-volume selection centered on the labeling slab, which is part of the standard pCASL implementation provided by the vendor. VSASL did not require any specific planning of the label. It should be noted that the gradient orientation for VS-labeling is coupled to the imaging volume coordinate system, meaning that those gradients experience the same angulation as the imaging volume. Consequently, also the VS-labeling gradients are aligned with or perpendicular to respiratory motion of the kidneys. Background suppression (BGS) was achieved by two hyperbolic secant inversion pulses played during the PLD. The inversion pulse timings were chosen based on simulation in MATLAB (Release 2015b, The MathWorks, Inc., Natick,

Massachusetts) considering kidney T_1-values from literature of 1057-1183 ms in the cortex and 1389-1573 ms in the medulla.[24] Depending on the PLD, BGS pulse timings were adapted to achieve a strong suppression of ~90% at the readout time of the first slice, without risking negative signal. Additionally, four WET (Water Excitation Technique) saturation pulses[25] were applied to the imaging region (presaturation) to eliminate residual magnetization modulation for the subsequent measurements. For VSASL, the presaturation module was inserted directly after the previous readout (Figure 2B); for pCASL, it was placed right before labeling.

3.3 | ASL Experiments

3.3.1 | Experiment 1: Velocity-selective labeling parameters and post-labeling delay

Kidneys of 15 healthy subjects (age 23-38, 6 men) were scanned using VSASL and pCASL (with 1500 ms label duration and 1500 ms PLD). To reduce the influence of motion, subjects were scanned during paced-breathing; subjects were asked to synchronize their breathing with the scanner noise, such that inhalation and exhalation were performed in the interval between image readout and the next labeling (Figure 2C). To allow for paced-breathing a TR of 6000 ms was chosen, resulting in a duration of 3:12 minutes per acquisition. In all subjects, a reference VSASL dataset using baseline settings was acquired. Baseline settings were chosen based on pilot experiments not reported in this work: V_c = 5.4 cm/s, gradient orientation = FH, PLD = 1200 ms. In addition, VS sequence parameters were systematically varied in five subjects each: cutoff velocity (2.1, 5.4, 10.7, 16.1 cm/s), labeling gradient orientation (FH, RL, AP) and post-labeling delay (400, 800, 1200, 1500 ms). For an overview of all acquired scans per subject, the reader is referred to Supporting Information Table S3. All VSASL acquisitions were performed for both sVSASL and dVSASL. BGS inversion pulse timings of the pCASL sequence were 1520/2600 ms, defined with respect to the end of the presaturation module. For VSASL with varying PLDs (400, 800, 1200, 1500 ms), the center of the inversion pulses were at 10/295, 10/640, 10/860, 10/1060 ms, respectively, defined from the end of the VS-labeling module (Supporting Information Table S3).

First, equilibrium magnetization images (M_0) were acquired without pCASL labeling and BGS and averaged over three repetitions. Next, pCASL data were acquired, followed by baseline VSASL and VS-labeling parameter variations. Subsequently, T_1 maps were acquired based on a cycled multi-slice inversion-recovery technique.[26] Finally, baseline VSASL was repeated (interval ~20 minutes).

3.3.2 | Experiment 2: Motion influence on velocity-selective label generation in the kidney

sVSASL datasets were collected from nine healthy subjects (age 26-34, three men) under free-breathing condition to study the influence of motion during labeling. With free-breathing, the TR could be reduced to 4500 ms. Respiratory motion was recorded using an external bellows. As we were primarily interested in the influence of bulk motion on VS-label generation, a simplified sequence with only a single VS-labeling module was used; this data was not analyzed in terms of RBF values. With a PLD of 1200 ms, V_c was varied (2.1-16.1 cm/s) for all labeling gradient orientations (FH, RL, AP), randomizing the scan order over subjects. In addition, M_0 and pCASL scans were acquired.

3.4 | Image analysis

All acquired data were stored as magnitude images and offline post-processing was done using MeVisLab (MeVis Medical Solutions AG, Bremen, Germany).

Retrospective motion correction was applied to all acquisitions of this study, regardless of the breathing strategy, for each kidney separately. The Elastix toolbox[27] was used with a B-Spline interpolator, an Adaptive Stochastic Gradient Descent optimizer and a B-Spline Stack transform. Using a PCA-based groupwise metric, the underlying cross-contrast registration problem introduced by BGS was accounted for.[28] Slice-wise registration input consisted of corresponding 2D images from all acquisitions per subject which were registered to a common space. Prior to image registration, input images were cropped to the size of the kidneys.

Voxel-wise T_1 was calculated by fitting a mono-exponential recovery function to the intensity of the 11 inversion-recovery images. Kidneys were manually segmented on the M_0-images of each subject. Segmentations were used as region of interest (ROI) for quality assessments, separately for left and right kidney. For Experiment 1, kidney ROIs were segmented semi-automatically into cortex, medulla, and rest (including the renal collecting system and veins). An intensity-based approach (Otsu's method[29]) was implemented to determine two thresholds for segmentation, based on the intensity values of the T_1 map, which were manually adapted if required. Further, no outlier rejection has been applied during analysis, neither on voxel nor on repetition basis.

3.4.1 | ASL quality metrics & quantification

ASL quality was assessed using three metrics: relative perfusion weighted signal (PWS), voxel-wise temporal

signal-to-noise ratio (tSNR), and quantitative RBF. Motion corrected label-control pairs were subtracted (ΔM) and averaged to calculate the PWS as a measure for the amount of generated label as $PWS = \Delta M / M_0 \times 100\%$. As a measure for precision, the voxel-wise tSNR was calculated as the ratio of the mean perfusion weighted signal over time ($\mu_{\Delta M}$) and the temporal standard deviation ($\sigma_{\Delta M}$); $tSNR = \mu_{\Delta M} / \sigma_{\Delta M}$. Reported tSNR and PWS were averaged over all voxels inside the kidney ROI for the left and right kidney.

For pCASL, RBF in mL/min/100 g was estimated using the general kinetic model by Buxton[11] for continuous ASL at a single PLD:

$$\Delta M = \frac{M_0 \cdot \alpha_{BGS}^n \cdot RBF \cdot T_{1t'} \cdot 2\alpha_{pCASL} \cdot e^{-ATT/T_{1b}} \cdot e^{-(PLD-BD-ATT)/T_{1t'}} \cdot \left(1 - e^{-BD/T_{1t'}}\right)}{6000 \cdot \lambda} \tag{1}$$

The apparent tissue relaxation T_{1t}, is given by $1/\left(1/T_{1t} + RBF/6000\lambda\right)$, with T_{1t} being the tissue T_1 and λ the blood partition coefficient. α_{pCASL}, the label pulse inversion efficiency, was set to 0.85.[7] The bolus duration (BD) equals the label duration of 1500 ms and the ATT was assumed to be 750 ms.[30] BGS inversion efficiency α_{BGS} was assumed to be 0.95, for each of the n BGS pulses applied. T_1 of arterial blood (T_{1b}) at 1.5T was set to 1350 ms.[7]

For VSASL, Buxton's pulsed ASL model for single time point measurements was adapted regarding three aspects. First, the diffusion attenuation error due to VS-labeling[19] in the label-condition is accounted for by adding the expected signal reduction $A_{diffusion}$ to ΔM, taking into account its T_1-decay during the PLD. Second, all of ΔM then experiences an additional scaling due to BGS efficiency α_{BGS}^n. Third, due to the application of a second VS-labeling module for venous crushing, both label and control image signal are attenuated; thus, the total ΔM is scaled by a factor β_{dual}, yielding Equation 2:

$$\Delta M = \alpha_{BGS}^n \cdot \beta_{dual} \left(M_0 \cdot \frac{RBF \cdot BD \cdot e^{-\frac{PLD}{T_{1b}}} \cdot q_p(PLD) \cdot \alpha_{VS}}{6000 \cdot \lambda} \right.$$
$$\left. + M_{0t} \cdot A_{diffusion} \cdot e^{-\frac{PLD}{T_{1t}}} \right) \tag{2}$$

with α_{VS} being the VS-labeling efficiency and BD the time between the two VS-labeling modules, and M_{0t} the equilibrium magnetization of tissue. The ATT is assumed to be negligible for VSASL as it is thought to label spins already inside the tissue. $q_p(PLD)$ is a dimensionless term as defined in Buxton et al Equation 3.[11] The derivation of Equation 2 can be found in the Supporting Information Appendix.

3.4.2 | Experiment 1: Velocity-selective labeling parameters and post-labeling delay

For the analysis of VS-labeling parameter effect on the ASL quality metrics, all data were included. The data used for subsequent investigation of VSASL sensitivity to renal perfusion were reviewed by visual inspection for repetitions with VS-labeling induced subtraction errors. Subjects in which these occurred were excluded from the calculation of RBF per kidney region.

All statistical analyses were performed using GraphPad Prism 8 version 8.0.1 (244) for Windows (GraphPad Software, San Diego California, USA). The effect of labeling parameter settings on global RBF, PWS, and tSNR was tested using non-parametric Friedman and Wilcoxon signed rank tests with a significance level of 0.05. To validate sensitivity of dVSASL to renal perfusion, segmented RBF values (global, cortex, medulla) were reported (baseline setting). Differences in RBF between regions as well as between the ASL techniques were tested for significance using paired Wilcoxon signed rank tests with $P < .05$. Bland-Altman analyses were performed to investigate the agreement of cortical RBF between VSASL (baseline setting) and pCASL. Evaluation of intra-session repeatability of renal dVSASL (baseline setting) on subject level was based on the within-session coefficient of variation (wsCV), calculated as the ratio of the within-session standard deviation ($\sigma_{\Delta M}$) and the mean ($\mu_{\Delta M}$); $wsCV = \sigma_{\Delta M} / \mu_{\Delta M}$.

3.4.3 | Experiment 2: Motion influence on velocity-selective label generation in the kidney

Analysis was done using MATLAB (Release 2015b, The MathWorks, Inc., Natick, Massachusetts, United States). The influence of motion on VS-label generation was analyzed for each kidney separately as they might move asynchronously. First, the start and end of the VS-labeling module and the respiratory bellows signal were extracted from the scanner log. The bellows response reflects motion of the abdominal wall and is usually interpreted to reflect respiratory phase. Here, bellows signal change between start and end of the VS-label provided a relative indicator for motion during the 50-ms VS-labeling module. Per subject, bellows signal change, was normalized to the maximum change found in the entire acquisition. The association of the average PWS over the entire kidney ROI with the bellows response was qualitatively assessed. Results

for VSASL acquisitions with different V_c were reported separately for the three labeling directions.

Three observers, blinded to the MRI acquisition settings, scored spurious label occurrence in the non-averaged (single subtraction) perfusion weighted images. A label-control pair was judged to contain spurious labeling when it showed homogeneously high ΔM over the entire kidney ROI (Supporting Information Figure S4). Per acquisition, for each kidney separately, ΔM maps of all repetitions (columns) and slices (rows) was presented to the observers. The scoring categories were: A, normal perfusion signal; B, might be; and C, definitely spuriously labeled. Finally, the number of spuriously labeled repetitions (assigned category C) was expressed as a percentage of the total number of repetitions.

Additionally, the paced-breathing (Experiment 1) and free-breathing (Experiment 2) PWS values were compared. Differences were tested for significance using unpaired Mann-Whitney tests with a significance level of 0.05.

4 | RESULTS

4.1 | Experiment 1: Velocity-selective labeling parameters and post-labeling delay

Data of all 15 subjects were included in the analysis of VS-labeling parameter effects on the ASL quality metrics. Representative examples of perfusion images obtained with VS-labeling are shown in Figure 3. Compared to the averaged control image, the signal was reduced upon VS-label application. The perfusion weighted image (ΔM) showed clear contrast between the highly perfused renal cortex and the low perfused medulla. As expected, an additional VS-labeling module right before the readout (dVSASL) reduced ΔM.

Figure 4 shows the influence of V_c, gradient orientation and PLD on the ASL quality metrics for global RBF, PWS, and tSNR. Separate RBF results for cortex and medulla can be found in the Supporting Information Figure S1. Cut-off velocity (Figure 4A): With decreasing V_c, the RBF increased for sVSASL ($P < .001$) but stayed nearly constant for dVSASL, only with the lowest V_c of 2 cm/s the RBF was significantly higher ($P = 0.006$). However, for both sVSASL and dVSASL at $V_c = 2.1$ cm/s, the intersubject variability increased considerably and subtraction errors were observed, identified as homogeneously high values over the entire kidney (Figure 5). PWS and tSNR both increased significantly for sVSASL but not for dVSASL with lower V_c. Gradient orientation (Figure 4B): Mean RBF, PWS, and tSNR calculated over all subjects, were only slightly affected by the labeling gradient orientation. Flow-sensitization in RL and AP yielded similar results for all metrics without significant
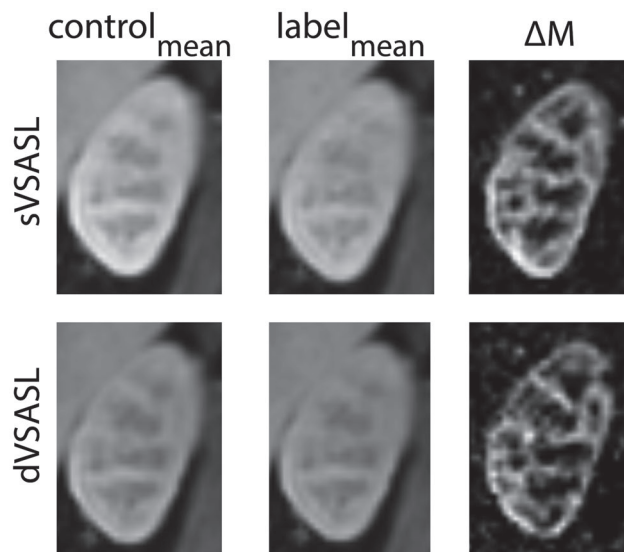

FIGURE 3 Center oblique coronal slice in the left kidney, showing sVSASL and dVSASL with baseline settings (PLD = 1200 ms, V_c = 5.4 cm/s, gradient orientation = FH). Motion-corrected and averaged control (left), label (middle) and subtraction ΔM images (right). From black to white intensity values are increasing; scaling of dVSASL ΔM is a factor 2 lower than sVSASL ΔM. Raw, unregistered, uncropped label and control images for all slices of one repetition are provided in Supporting Information Figure S5

difference. FH-labeling resulted in the highest RBF, PWS, and tSNR values for all subjects. For sVSASL, however, FH-labeling also increased the variation between subjects compared to labeling in the other orientations. For this setting subtraction errors occurred in two of five subjects, which could affect intersubject variability. dVSASL was less dependent on labeling orientation, both in terms of mean values as variability. PLD (Figure 4C): For sVSASL, RBF, PWS, and tSNR steadily decreased with increasing PLD ($P < .05$). Particularly high RBF and PWS were observed for short PLDs ($\leq$800 ms) in the kidney pedicle and mainly for sVSASL (Supporting Information Figure S2). These findings coincided with a high tSNR since this high signal was stable over all repetitions. The observed high values might originate from undesired label, generated in large vessels, including veins, as well as the renal collecting system, and were seen to decrease with longer PLD. Varying the PLD had a much smaller effect on dVSASL, for which RBF was slightly higher for PLD around 400 ms ($P < .05$), but the tSNR was lower ($P > .05$). An outlier is present for dVSASL at a PLD of 400 ms with extremely high RBF, PWS, and tSNR. Review of the source images indicated subtraction errors in 10/15 repetitions, possibly induced by motion, as non-compliance with the paced-breathing protocol was indicated by the subject. The highest tSNR for dVSASL was found with PLD = 1200 ms ($P > .05$). For sVSASL, maximum RBF, PWS, and tSNR occurred at short delays (PLD $\leq$ 800 ms).
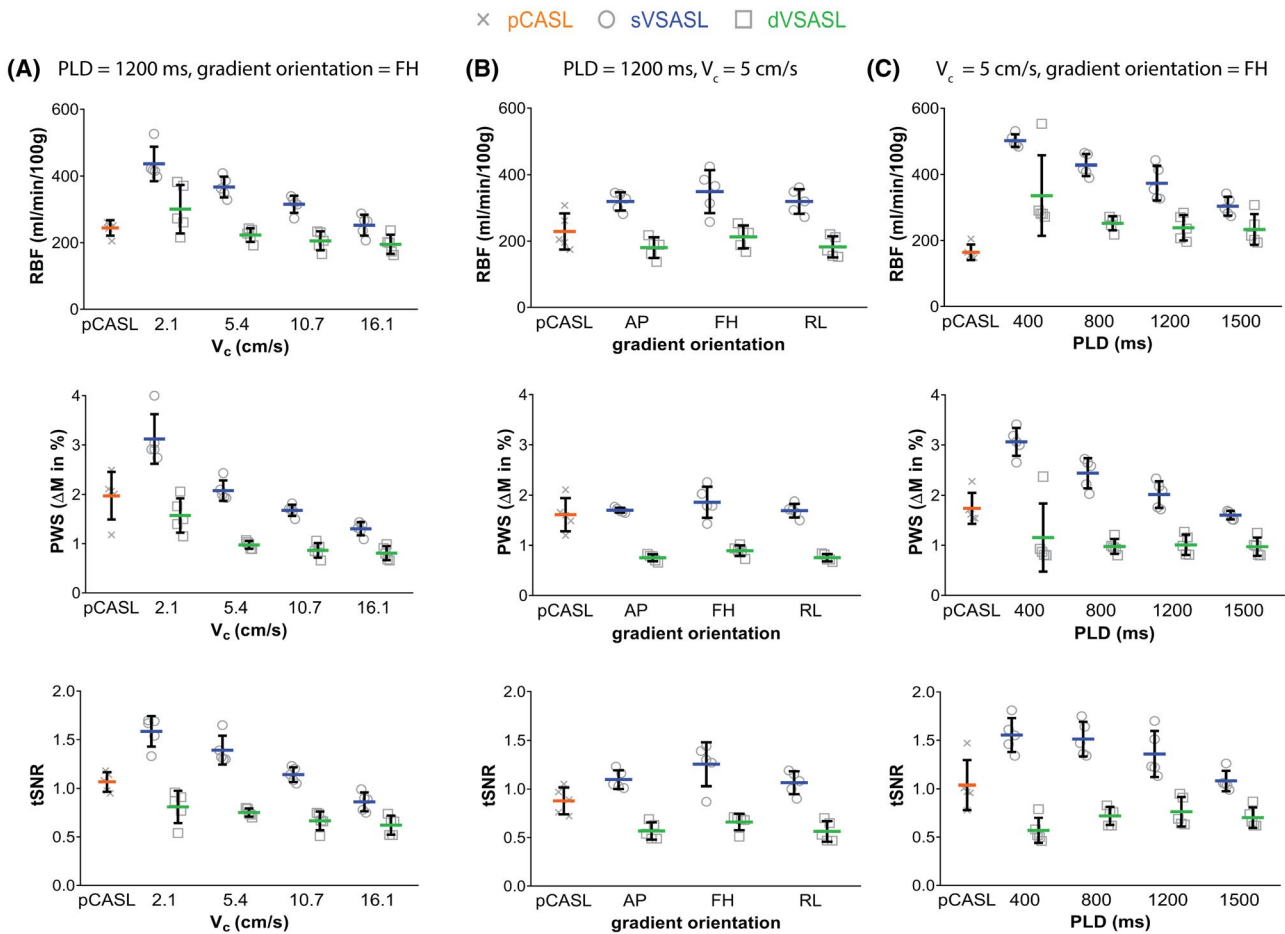
FIGURE 4 Individual global RBF, PWS, and tSNR (tSNR) as a function of varying sequence parameters; cutoff velocity V_c (A), labeling gradient orientation (B), and post-labeling delay PLD (C). Results for pCASL, sVSASL, and dVSASL are presented. Data points are shown on subject level. Horizontal bars represent mean values. Error bars (vertical lines) denote standard deviation; for RBF and PWS representing intersubject variability whereas for the tSNR they rather reflect variability of the intrasubject signal robustness
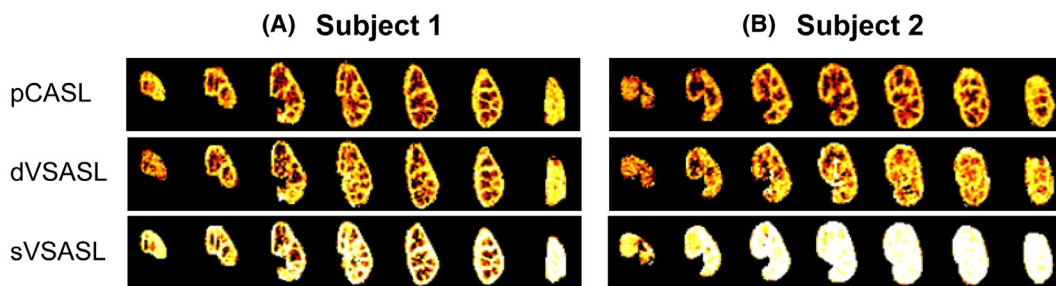

FIGURE 5 Masked RBF maps for all seven slices of the left kidney acquired with baseline setting VSASL in single and dual fashion for two subjects. For comparison, the reference pCASL is shown as well. (A) Subject without subtraction errors. (B) Subject with subtraction errors in 2 of 15 repetitions corrupting the sVSASL perfusion map, resulting in homogeneously high erroneous perfusion values

Overall, baseline VSASL had similar tSNR as pCASL, with somewhat higher values for sVSASL (1.36 ± 0.21) ($P < .05$) and lower values for dVSASL (0.71 ± 0.10) ($P > .05$) than pCASL (1.04 ± 0.19). For PWS, a similar pattern emerged.

For validation of dVSASL (baseline setting) sensitivity to renal perfusion, 5 of the 15 subjects were excluded due to

VS-labeling induced subtraction errors. For RBF values of excluded subjects, see Supporting Information Table S2. Figure 6 shows RBF per kidney region for all ASL techniques. RBF for sVSASL was highest in all regions, which is expected due to venous contributions and unknown bolus-width (Figures 4 and S2). Consequently, sVSASL was excluded from further analysis. RBF measured with dVSASL and pCASL
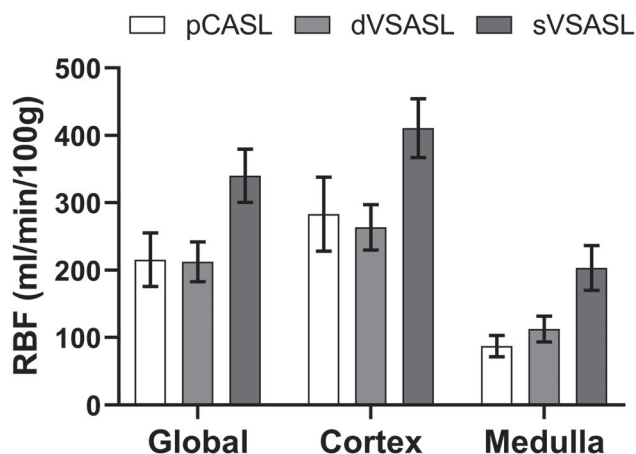
FIGURE 6 Mean RBF values measured with baseline dVSASL, sVSASL, and pCASL in different kidney regions (global, cortex, and medulla) for 10 included subjects. Error bars indicate standard deviation
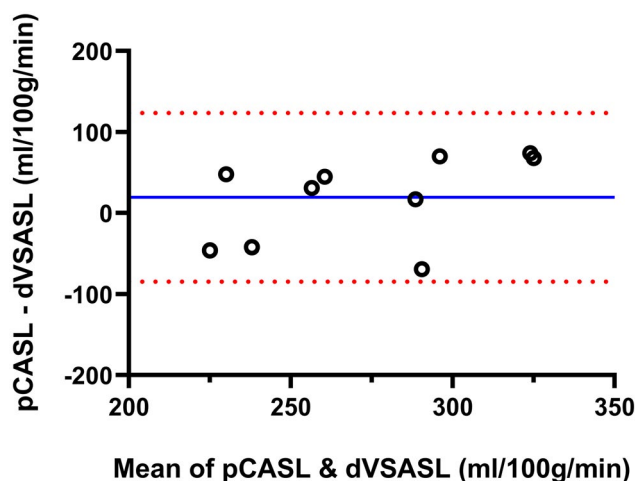

FIGURE 7 Bland-Altman plot of cortical RBF values measured with pCASL and dVSASL (baseline setting) for 10 included subjects. Solid blue line and dotted red lines represent the mean difference and 95% limits of agreement, respectively

was consistently higher in the cortex than in the medulla ($P = .002$). For cortical perfusion, pCASL measured on average 7% higher RBF values than dVSASL ($P = .28$): the average cortical RBF across subjects for baseline dVSASL was 264 ± 34 mL/min/100 g and for pCASL 283 ± 55 mL/min/100 g; with a 38% lower intersubject variability with dVSASL. In the medulla, pCASL RBF values were 22% lower than with dVSASL ($P = .004$). The Bland-Altman analysis of cortical RBF measured with dVSASL (baseline setting) and pCASL (Figure 7) revealed a bias of 19.6 mL/min/100 g without a systematic trend, but showed relatively wide limits of agreement at -84.5 mL/min/100 g and 123.7 mL/min/100 g, related to substantial differences on the individual level. The wsCV of cortical RBF for baseline dVSASL was 4.5% (for wsCV on subject level; see Supporting Information Figure S3).

4.2 | Experiment 2: Motion influence on velocity-selective label generation in the kidney

MRI data and bellows signal from nine subjects were collected; however, due to poor bellows signal quality (signal gaps, interruption), only six subjects were included for analysis.

Figure 8 shows the PWS versus bellows signal change for acquisitions with varying V_c's in different labeling gradient orientations. With labeling in the respiratory FH direction and a low V_c of 2.1 cm/s, label-control pairs with extremely high PWS were observed. For higher V_c this occurred less frequently. With RL-labeling, a slightly elevated PWS can be observed for $V_c = 2.1$ cm/s, whereas with AP-labeling this effect is hardly visible. In all experiments, respiratory motion during VS-labeling was present, as documented by the change in bellows signal. Still, we found no one-to-one correlation between respiratory bellows signal change and generated spurious label. Comparing data from free-breathing and paced-breathing from Experiments 1 and 2 in Figure 8D, we found that FH-labeling generated significantly more spurious label during free-breathing than during paced-breathing, but only at a low V_c of 2.1 cm/s ($P = .0159$), further supporting the association of spurious labeling with respiratory motion.

The dependence of the generated PWS is also readily apparent from the averaged PWS images for varying V_c and VS-labeling orientations; see Figure 9. Exceptionally high, homogeneous PWS in the entire kidney ROI without cortico-medullary contrast is seen for FH-labeling with $V_c = 2.1$ cm/s, whereas this effect is almost absent for RL- or AP-labeling, and substantially lower for encoding with higher cutoff velocity.

There was no significant difference in subtraction error occurrence between left and right kidney. Thus, subtraction error scores were averaged for the three observers and summarized for both kidneys (Supporting Information Table S1). Subtraction error occurrence was highest for labeling with $V_c = 2.1$ cm/s. On average 25.4% of the repetitions showed subtraction errors with FH-labeling. Changing the gradient orientation to RL and AP reduced subtraction errors to 4.3% and 4.9%, respectively. With increasing V_c, repetitions with subtraction error occurred less frequently and were no longer observed for FH-labeling at 16.1 cm/s, RL-labeling at 10.7 cm/s and AP-labeling already at 5.4 cm/s, respectively.

Moreover, in addition to extremely positive signal inside the kidney ROI, all three observers observed patches of negative signal for a few repetitions (Supporting Information Figure S4). However, their occurrence was not included in the scoring task as the observers were not instructed for those.

5 | DISCUSSION

In this work, we demonstrated the feasibility of VSASL for renal perfusion measurement and explored the influence of
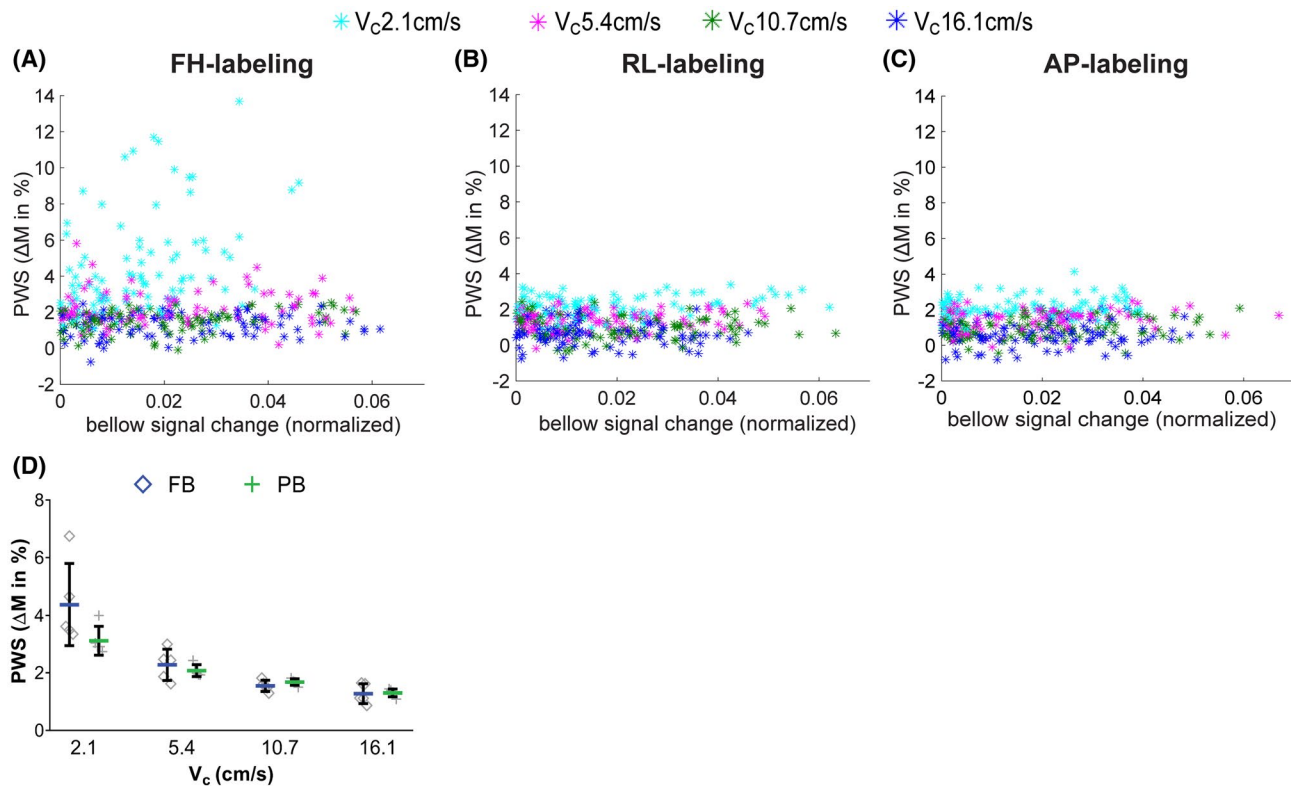
FIGURE 8 Generated label, ie, control-label subtraction, averaged over the entire kidney ROI as a function of the respiratory bellows signal change during VS-labeling. Data are shown for the left kidney of five subjects, with one data point per repetition, for FH-labeling (A), RL-labeling (B), and AP-labeling (C), respectively. Per subject, the bellows signal was normalized to the maximum range of that subject. The marker color indicates cutoff velocities; $V_c = 2.1$ (cyan), $V_c = 5.4$ (pink), $V_c = 10.7$ (green), $V_c = 16.1$ cm/s (blue). (D) PWS for acquisitions with varying V_c under PB (green plus) versus FB (blue diamond) from Experiment 1 and 2, respectively. Note, FB and PB results are from different subjects. From Experiment 1 PB data were available from five subjects with varying V_c in FH direction; hence, for this comparison, FB data of five of nine subjects was randomly selected from Experiment 2

essential parameters for VS labeling as well as the influence of (respiratory-) kidney motion on VS-label generation. We found that labeling parameters had a substantial effect on the generated label, as well as on the sensitivity to labeling artifacts. With lower cutoff velocity, the perfusion signal and tSNR increased significantly, but also the frequency of spurious tissue labeling. Changing the labeling gradient orientation had a smaller but still significant effect, with FH-labeling giving the highest PWS and tSNR, but also the highest labeling artifact occurrence. Systematic investigation of the VS-label generation sensitivity to kidney motion showed a dependence on gradient orientation and cutoff velocity. In combination with a free-breathing sVSASL experiment with motion monitoring using the respiratory bellows, we showed that spurious labeling occurrence was associated with respiratory motion. By choosing a direction where respiratory motion is less dominant, eg, AP or RL, motion-induced VS-labeling artifacts were fully eliminated with $V_c \geq 10.7$ cm/s. In addition, results showed an effect of PLD on label dynamics, as for sVSASL the signal and tSNR decreased with longer PLD, whereas for dVSASL, perfusion signal and tSNR were

highest for a PLD of 1200 ms. Finally, we compared cortical RBF measured with dVSASL with the reference pCASL and found slightly lower RBF and tSNR.

In the kidney, we have to balance the efficiency and location of label creation with the occurrence of labeling artifacts related to (respiratory) motion during the VS-labeling module(s). The issue of motion-induced tissue labeling at low V_c has already been raised when VSASL was first introduced for the brain[13] and more recently for the myocardium,[17] but has not been demonstrated in vivo. In this study, we indeed observed that its occurrence was highest for $V_c = 2.1$ cm/s with FH-labeling, the dominant direction of respiratory motion. With higher V_c and RL- or AP-labeling, the occurrence was reduced. High V_c also means label is generated more upstream, yet, with a V_c of 10.7 cm/s it is expected to reach as far as the interlobar arteries, where velocities of about 28 cm/s have been found.[31] The PLD should be chosen sufficiently long to allow enough arterial spins to decelerate before the second VS-labeling module is applied, but also short enough to avoid signal decay. With a PLD of 1200 ms we found highest RBF and tSNR for baseline dVSASL, which is in line with
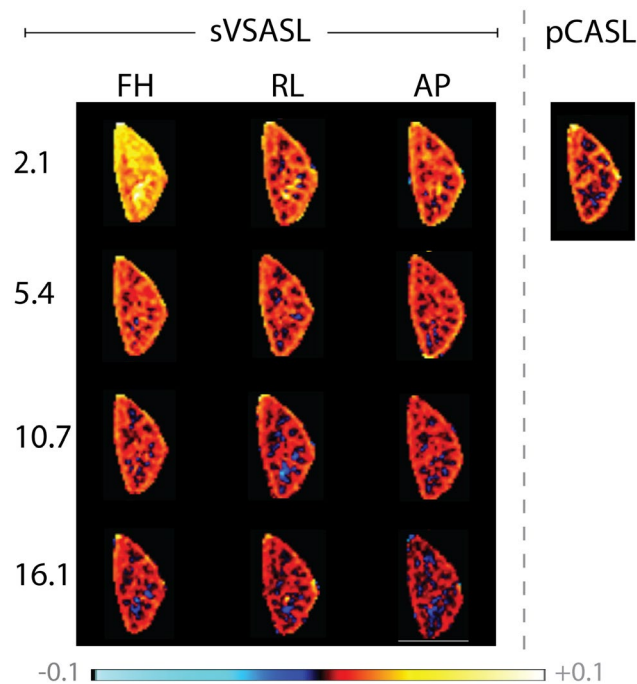
FIGURE 9 Averaged perfusion weighted signal in a single slice of the left kidney. Label was generated with a single VS-labeling module at four different V_c (rows) with three different velocity encoding directions (columns). pCASL is shown for comparison (right)

the observation that the labeled blood requires time to accumulate and decelerate in order to avoid saturation by the second VSASL module. Consequently, we would recommend a conservative VS-parameter choice, meaning RL or AP labeling with a V_c of 10.7 cm/s and a PLD of 1200 ms. Still, those values might differ under pathological conditions in patient populations and could profit from further investigation.

We found no one-to-one correlation between motion amplitude and spurious tissue labeling at the level of individual repetitions. Some repetitions had tissue labeling without the bellows indicating motion, others showed no spurious labeling even when motion was detected. Several mechanisms can play a role here. First, moving tissue magnetization shows a sinusoidal dependence on velocity, rather than having a cutoff velocity above which saturation takes place, such as for the laminar flow in a vessel. Second, with the bellows we were not able to probe kidney velocity directly. Direct kidney motion estimation could be improved with internal surrogates, eg, image navigators, but those would affect the sequence and were therefore not used.

In Experiment 1 spurious labeling was observed in 5 of 15 subjects. Those subjects mentioned difficulties in paced-breathing compliance, supporting that just paced-breathing is insufficient for motion compensation, and that still a higher V_c with a non-FH labeling gradient orientation is required in clinical studies to avoid spurious tissue labeling.

For dVSASL, spurious labeling can also occur in the control images. As in the dVSASL control condition only the second module includes flow-sensitizing gradients, the probability of spurious labeling in control images (resulting in extremely negative PWS) is half of the probability of spurious labeling in label images (resulting in extremely positive PWS). Either a sufficiently high V_c will resolve this issue or outlier rejection based on the source images would prevent repetitions with spurious label in control and label images from corrupting the resulting RBF maps.

To avoid impairment of the small ASL signal due to aliasing artifacts, we used saturation slabs superior and inferior to the FOV. With that, blood outside the FOV is saturated which is intended to be labeled during the next TR. Therefore, a sufficiently long recovery delay from the previous TR until labeling of the subsequent TR needs to be assured. In our implementation this was achieved by a TR that included a recovery delay of 2 times $T1_b$.

A single VS-labeling module labels both arterial and venous blood, which can explain the extremely high signal in the kidney center, especially for short PLD (<800 ms), therefore limiting their quantitative interpretation for renal perfusion measurement. However, sVSASL still has potential for research purposes to monitor and understand VS label-generation. Nevertheless, for renal ASL the generated VS-label should be restricted to arterial blood to obtain a quantitative perfusion signal. Undesired venous signal can be eliminated with the application of a second VS-labeling module (dVSASL),[14] as supported by our results where a short PLD only yields extremely high PWS values for sVSASL but not for dVSASL (Supporting Information Figure S2).

The cortical RBF values for baseline dVSASL (264 $\pm$ 34 mL/min/100 g) and pCASL (283 $\pm$ 55 mL/min/100 g) were in agreement with previous reports. Robson et al[32] also performed pCASL with BGS and paced-breathing on 1.5T and reported cortical RBF values of 284 $\pm$ 21 mL/min/100 g. Similar values of 310 $\pm$ 10 mL/min/100 g were found by Gardener and Francis[33] with the application of respiratory triggered Flow-sensitive Alternating Inversion Recovery (FAIR). More recently, Taso et al[34] reported cortical RBF values between 286-316 mL/min/100 g under free-breathing at 3T. Likewise, our results on repeatability were comparable to previous reports with an average wsCV in cortical RBF of 3.5% for dVSASL for acquisitions 20 minutes apart. Robson et al[32] found a within-session repeatability of global RBF of 8%, using pCASL at 1.5T; Kim et al,[35] reported a within-subject CV in cortical RBF of 14.4%, under breathing instructions with breath hold for pCASL at 3T. Still, dVSASL yielded 30% lower tSNR than pCASL. This could be explained by the VS-preparation that ideally saturates spins whereas pCASL works with inversion. dVSASL tSNR could be improved by employing the recently proposed VS-inversion technique.[16]

Cortical RBF as well as intersubject variability were lower for dVSASL than for pCASL, without significant difference. This could either indicate insensitivity to perfusion changes or higher precision. Differences on subject level between dVSASL and pCASL have been observed (Figure 7), but did not follow a systematic trend. Examinations in patients or healthy subjects with a challenge that alters kidney perfusion such as food intake[36,37] would be required to confirm sensitivity to perfusion changes. In addition, it should be noted that quantification of VSASL data was performed to the best of our knowledge; as previously done,[13,15,17] Buxton's kinetic model for pulsed ASL was used plus we included corrections for diffusion weighting errors and the application of a second VS-labeling module. Still, the applicability of this model for VSASL in the kidney needs to be further demonstrated and could be subject of further investigation.

VSASL has several attractive features for renal perfusion measurement, including insensitivity to ATT, which would allow for accurate quantification even with single PLD measurements. Here, ATT insensitivity was not yet demonstrated, but could be evaluated in multi-PLD experiments.[38,39] Moreover, by obviating the need for label planning as compared to spatial labeling techniques, VSASL is a highly attractive candidate for clinical introduction.

6 | CONCLUSIONS

We demonstrated the feasibility of VSASL for renal perfusion measurement. With properly chosen sequence parameters, such as VS-labeling module cutoff velocity and labeling gradient orientation, challenges such as spurious labeling due to respiratory motion can be minimized while obtaining efficient blood labeling. Dual VSASL provided perfusion maps showing corticomedullary contrast with slightly lower tSNR and mean perfusion values in the renal cortex than pCASL. VSASL could ultimately offer a planning-free, non-invasive technique with less dependence on altered ATT, such as found in elderly and renal patient population.

CONFLICT OF INTEREST
Marijn van Stralen: Co-founder and shareholder of MRIguidance B.V.

ETHICS
Approval from the institutional review board, and written informed consent from all subjects were obtained.

ORCID
Isabell K. Bones https://orcid.org/0000-0002-7916-5013
Suzanne L. Franklin https://orcid.org/0000-0001-6886-5578
Anita A. Harteveld https://orcid.org/0000-0002-3379-0710
Matthias J. P. van Osch https://orcid.org/0000-0001-7034-8959
Jeroen Hendrikse https://orcid.org/0000-0001-6384-6140
Chrit Moonen http://orcid.org/0000-0001-5593-3121
Marijn van Stralen https://orcid.org/0000-0002-3051-5000
Clemens Bos https://orcid.org/0000-0002-9246-3242

REFERENCES
1. Selby NM, Blankestijn PJ, Boor P, et al. Magnetic resonance imaging biomarkers for chronic kidney disease: A position paper from the European cooperation in science and technology action PARENCHIMA. *Nephrol Dial Transplant*. 2018;33(suppl_2):ii4–ii14.
2. Beierwaltes WH, Harrison-Bernard LM, Sullivan JC, Mattson DL. Assessment of renal function; clearance, the renal microcirculation, renal blood flow, and metabolic balance. *Compr Physiol*. 2013;3:165–200.
3. Odudu A, Nery F, Harteveld AA, et al. Arterial spin labelling MRI to measure renal perfusion: A systematic review and statement paper. *Nephrol Dial Transplant*. 2018;33(suppl_2): ii15–ii21.
4. Wong EC. An introduction to ASL labeling techniques. *J Magn Reson Imaging*. 2014;40:1–10.
5. Jahanian H, Noll DC, Hernandez-Garcia L. B0 field inhomogeneity considerations in pseudo-continuous arterial spin labeling (pCASL): Effects on tagging efficiency and correction strategy. *NMR Biomed*. 2011;24:1202–1209.
6. Aslan S, Xu F, Wang PL, et al. Estimation of labeling efficiency in pseudocontinuous arterial spin labeling. *Magn Reson Med*. 2010;63:765–771.
7. Alsop DC, Detre JA, Golay X, et al. Recommended implementation of arterial spin-labeled Perfusion MRI for clinical applications: A consensus of the ISMRM perfusion study group and the European consortium for ASL in dementia. *Magn Reson Med*. 2015;73:102–116.
8. Campbell AM, Beaulieu C. Pulsed arterial spin labeling parameter optimization for an elderly population. *J Magn Reson Imaging*. 2006;23:398–403.
9. Liu Y, Zhu X, Feinberg D, et al. Arterial spin labeling MRI study of age and gender effects on brain perfusion hemodynamics. *Magn Reson Med*. 2012;68:912–922.
10. Richter CS, Krestin GP, Eichenberger AC, Schöpke W, Fuchs WA. Assessment of renal artery stenosis by phase-contrast magnetic resonance angiography. *Eur Radiol*. 1993;3:493–498.

11. Buxton RB, Frank LR, Wong EC, Siewert B, Warach S, Edelman RR. A general kinetic model for quantitative perfusion imaging with arterial spin labeling. *Magn Reson Med*. 1998;40:383–396.

12. Norris DG, Schwarzbauer C. Velocity selective radiofrequency pulse trains. *J Magn Reson*. 1999;137:231–236.

13. Wong EC, Cronin M, Wu WC, Inglis B, Frank LR, Liu TT. Velocity-selective arterial spin labeling. *Magn Reson Med*. 2006;55:1334–1341.

14. Duhamel G, De Bazelaire C, Alsop DC. Evaluation of systematic quantification errors in velocity-selective arterial spin labeling of the brain. *Magn Reson Med*. 2003;50:145–153.

15. Schmid S, Heijtel DFR, Mutsaerts HJMM, et al. Comparison of velocity- and acceleration-selective arterial spin labeling with [15O]H2O positron emission tomography. *J Cereb Blood Flow Metab*. 2015;35:1296–1303.

16. Qin Q, van Zijl PCM. Velocity-selective-inversion prepared arterial spin labeling. *Magn Reson Med*. 2016;76:1136–1148.

17. Jao TR, Nayak KS. Demonstration of velocity selective myocardial arterial spin labeling perfusion imaging in humans. *Magn Reson Med*. 2017;80:272–278.

18. Zun Z, Limperopoulos C. Placental perfusion imaging using velocity-selective arterial spin labeling. *Magn Reson Med*. 2018;80:1036–1047.

19. Schmid S, Ghariq E, Teeuwisse WM, Webb A, Van Osch MJP. Acceleration-selective arterial spin labeling. *Magn Reson Med*. 2014;71:191–199.

20. Sulkowska K, Palczewski P, Duda-Zysk A, et al. Diffusion-weighted MRI of kidneys in healthy volunteers and living kidney donors. *Clin Radiol*. 2015;70:1122–1127.

21. Wu WC, Wong EC. Feasibility of velocity selective arterial spin labeling in functional MRI. *J Cereb Blood Flow Metab*. 2007;27:831–838.

22. Stanisz GJ, Odrobina EE, Pun J, et al. T1, T2 relaxation and magnetization transfer in tissue at 3T. *Magn Reson Med*. 2005;54:507–512.

23. Wu WC, Fernández-Seara M, Detre JA, Wehrli FW, Wang J. A theoretical and experimental investigation of the tagging efficiency of pseudocontinuous arterial spin labeling. *Magn Reson Med*. 2007;58:1020–1027.

24. Huang Y, Sadowski EA, Artz NS, et al. Measurement and comparison of T1 relaxation times in native and transplanted kidney cortex and medulla. *J Magn Reson Imaging*. 2011;33:1241–1247.

25. Ogg RJ, Kingsley PB, Taylor JS. WET, a T1- and B1-insensitive water-suppression method for in vivo localized 1H NMR spectroscopy. *J Magn Reson Ser B*. 1994;104:1–10.

26. Clare S, Jezzard P. Rapid T1 mapping using multislice echo planar imaging. *Magn Reson Med*. 2001;45:630–634.

27. Klein S, Staring M, Murphy K, Viergever MA, Pluim J. elastix: A toolbox for intensity-based medical image registration. *IEEE Trans Med Imaging*. 2010;29:196–205.

28. Huizinga W, Poot D, Guyader J-M, et al. PCA-based groupwise image registration for quantitative MRI. *Med Image Anal*. 2016;29:65–78.

29. Hima Bindu C, Satya PK. An efficient medical image segmentation using conventional OTSU method. *Int J Adv Sci Technol*. 2012;38(November):67–74.

30. Roberts DA, Detre JA, Bolinger L, et al. Renal perfusion in humans: MR imaging with spin tagging of arterial water. *Radiology*. 1995;196:281–286.

31. Deeg KH, Wörle K, Wolf A. Dopplersonographische Bestimmung von altersabhängigen Normalwerten der Flussgeschwindigkeiten und des Resistance-Index in den Nierenarterien gesunder Kinder. *Ultraschall der Medizin*. 2003;24:312–322.

32. Robson PM, Madhuranthakam AJ, Dai W, Pedrosa I, Rofsky NM, Alsop DC. Strategies for reducing respiratory motion artifacts in renal perfusion imaging with arterial spin labeling. *Magn Reson Med*. 2009;61:1374–1387.

33. Gardener AG, Francis ST. Multislice perfusion of the kidneys using parallel imaging: Image acquisition and analysis strategies. *Magn Reson Med*. 2010;63:1627–1636.

34. Taso M, Guidon A, Alsop DC. Influence of background suppression and retrospective realignment on free-breathing renal perfusion measurement using pseudo-continuous ASL. *Magn Reson Med*. 2019;81:2439–2449.

35. Kim DW, Shim WH, Yoon SK, et al. Measurement of arterial transit time and renal blood flow using pseudocontinuous ASL MRI with multiple post-labeling delays: Feasibility, reproducibility, and variation. *J Magn Reson Imaging*. 2017;46:813–819.

36. Deibert P, Lutz L, König D, et al. Acute effect of a soy protein-rich meal-replacement application on renal parameters in patients with the metabolic syndrome. *Asia Pac J Clin Nutr*. 2011;20:527–534.

37. Chan AYM, Cheng MLL, Keil LC, Myers BD. Functional response of healthy and diseased glomeruli to a large, protein-rich meal. *J Clin Invest*. 1988;81:245–254.

38. Qiu D, Straka M, Zun Z, Bammer R, Moseley ME, Zaharchuk G. CBF measurements using multidelay pseudocontinuous and velocity-selective arterial spin labeling in patients with long arterial transit delays: Comparison with xenon CT CBF. *J Magn Reson Imaging*. 2012;36:110–119.

39. Guo J, Meakin JA, Jezzard P, Wong EC. An optimized design to reduce eddy current sensitivity in velocity-selective arterial spin labeling using symmetric BIR-8 pulses. *Magn Reson Med*. 2015;73:1085–1094.

SUPPORTING INFORMATION

Additional Supporting Information may be found online in the Supporting Information section.

FIGURE S1 Individual renal blood flow (RBF) for (A) cortex and (B) medulla as a function of varying sequence parameters. Error-bars reflect intersubject variability which is independent from measurement precision and accuracy. Results for pCASL, single VSASL (sVSASL) and dual VSASL (dVSASL) are presented

FIGURE S2 PWIs for a center slice of the right kidney of one subject with varying PLDs (400, 800, 1200, 1500 ms) acquired with sVSASL and dVSASL. High signal in the kidney center appeared for sVSASL at short PLD (≤800 ms), as indicated by the blue arrow, while this was not apparent for dVSASL

FIGURE S3 Within session coefficient of variation (wsCV (%)) of cortical RBF for both kidneys on subject level acquired with single- and dual VSASL using baseline settings. Subjects with VS-labeling induced subtraction errors were excluded. Intersubject variation is represented by the vertical error bars

FIGURE S4 Registered label and control images of dVSASL with the corresponding perfusion weighted images (PWIs) for one slice of one subject before averaging. Example of

repetitions with highly positive signal (yellow square) as can be seen in repetition 6 and 13 as well as for negative signal (blue square) as for repetition 2. In contrast, sVSASL and pCASL PWIs did not contain subtraction errors due to spurious tissue labeling. The authors speculate that the remarkable cortex and medulla contrast in raw label and control images (blue and yellow square) originates from T1 differences between cortex and medulla which play a role after the partial inversion by the VS-labeling module. In the absence of motion, the VS-labeling module only results in a slight reduction of the longitudinal magnetization, without introducing tissue contrast

FIGURE S5 Example full field-of-view source images of one subject acquired during paced-breathing. (A) label and control images for baseline sVSASL, dVSASL and pCASL of all 7 slices for one repetition. (B) M0 images of one repetition; intensity scaling doubled. (C) Seven different inversion times out of eleven for T1-mappping shown for a single slice

FIGURE S6 Example for FOV (green box) and pseudo-continuous ASL (pCASL) label slab planning (blue box)

TABLE S1 Average % of definitely spuriously labeled repetitions summarized for both kidneys based on three observers for all available acquisitions with varying cutoff velocity V_c in cm/s (rows) and gradient orientation (columns) for single- and dual VSASL. As dual VSASL was only performed in experiment 1, where not all Vc combinations were scanned in each direction, settings without acquisitions are indicated with not available (NA)

TABLE S2 Cortical RBF values achieved using baseline dual VSASL (FH-labeling, PLD = 1200 ms, V_c = 5 cm/s) and the according spurious label occurrence for all subjects. Spurious label occurrence is given as number of affected repetitions per acquisition. Grey indicating excluded subjects from cortical RBF calculation

TABLE S3 VSASL parameter variation scans acquired per subject. All variation scans were acquired two times, with single and dual VSASL. Bold numbers indicating baseline settings